Molecular Neurobiology
https://doi.org/10.1007/s12035-019-01839-8

Progerin-Induced Transcriptional Changes in Huntington's Disease Human Pluripotent Stem Cell-Derived Neurons

Dorit Cohen-Carmon[1] · Matan Sorek[1,2] · Vitaly Lerner[2,3] · Mundackal S. Divya[1,4] · Malka Nissim-Rafinia[1] · Yosef Yarom[2,3] · Eran Meshorer[1,2]

Received: 13 September 2019 / Accepted: 14 November 2019

Abstract

Huntington's disease (HD) is a neurodegenerative late-onset genetic disorder caused by CAG expansions in the coding region of the Huntingtin (*HTT*) gene, resulting in a poly-glutamine (polyQ) expanded HTT protein. Considerable efforts have been devoted for studying HD and other polyQ diseases using animal models and cell culture systems, but no treatment currently exists. Human embryonic stem cells (ESCs) and induced pluripotent stem cells (iPSCs) offer an elegant solution for modeling human diseases. However, as embryonic or rejuvenated cells, respectively, these pluripotent stem cells (PSCs) do not recapitulate the late-onset feature of the disease. Here, we applied a robust and rapid differentiation protocol to derive electrophysiologically active striatal GABAergic neurons from human wild-type (WT) and HD ESCs and iPSCs. RNA-seq analyses revealed that HD and WT PSC-derived neurons are highly similar in their gene expression patterns. Interestingly, ectopic expression of Progerin in both WT and HD neurons exacerbated the otherwise non-significant changes in gene expression between these cells, revealing IGF1 and genes involved in neurogenesis and nervous system development as consistently altered in the HD cells. This work provides a useful tool for modeling HD in human PSCs and reveals potential molecular targets altered in HD neurons.

Keywords Progerin · iPS cells · iPSC · Neuronal differentiation · Embryonic stem cells · HD

Introduction

Huntington's disease (HD) is a dominant late-onset genetic disorder characterized by neurodegeneration of the striatum and cortex, with symptoms of physical, behavioral, and mental disabilities [1]. Although the CAG-repeat/poly-glutamine (PolyQ) mutation in the Huntingtin (HTT) gene causing HD has been described over 25 years ago [2, 3], no cure or effective therapies are yet available. Alongside the various non-human animal model systems available, each with its own limitations [4], the study of HD has been recently pushed forward by the use of human pluripotent stem cell (PSC) model systems [5]. PSCs have a dual capacity to self-renew indefinitely and to differentiate to any cell type, and as such, can establish a variety of cellular models for many different human diseases [6]. PSCs include human embryonic stem cells (hESCs) derived from preimplantation genetic diagnosis (PGD) embryos, as well as human induced pluripotent stem cells (iPSCs), derived by reprogramming patient somatic cells [7]. Both such systems enable to explore disease mechanisms in culture. In HD, the first neurons to be damaged are medium spiny neurons (MSNs), a unique type of GABAergic neurons in the striatum in the basal ganglia [8].

Existing GABAergic differentiation protocols are limited in their capacity mainly due to long and cumbersome procedures (60–80 days), low differentiation efficiency (<~ 20%), and challenges in obtaining pure neuronal culture without other

Dorit Cohen-Carmon and Matan Sorek contributed equally to this work.

Electronic supplementary material The online version of this article (https://doi.org/10.1007/s12035-019-01839-8) contains supplementary material, which is available to authorized users.

✉ Eran Meshorer
eran.meshorer@mail.huji.ac.il

[1] Department of Genetics, The Alexander Silberman Institute of Life Sciences, Edmond J. Safra Campus, The Hebrew University of Jerusalem, 91904 Jerusalem, Israel

[2] The Edmond and Lily Safra Center for Brain Sciences, Edmond J. Safra Campus, The Hebrew University of Jerusalem, 91904 Jerusalem, Israel

[3] Department of Neurobiology, The Alexander Silberman Institute of Life Sciences, Edmond J. Safra Campus, The Hebrew University of Jerusalem, 91904 Jerusalem, Israel

[4] Department of Pathology, Sree Chitra Tirunal Institute for Medical Sciences and Technology, Thiruvananthapuram 695011, Kerala, India

Published online: 13 December 2019

CNS-related cells [9–12]. We therefore set out to develop a relatively short, effective, and reproducible protocol. Considering the natural processes that underlie GABAergic neuronal development, and based on existing protocols [9, 10, 12], we conducted a series of calibration and optimization experimentations of different combinations of neurofactors. We were able to optimize a differentiation protocol, which does not require colony or rosette picking, no animal-based cell feeders nor sorting. This protocol generates a relatively high yield (~40%) of striatal GABAergic post-mitotic neurons within 45 days. The obtained neurons express GABAergic and striatal marker combinations, display electrophysiological properties of GABA receptor containing neurons, and are successfully grafted for several months in striatal Quinolinic Acid (QA) lesioned mice. Using transcriptional profiles of both "young" and "aged" [13] WT and HD neurons, combining data from more than 10 cell lines of both iPSC- and hESC-derived neurons, we identified disease-associated genes, providing potential pathways for pharmacological intervention.

Materials and Methods

Cell Lines and Genotyping

The following hESCs (from PGDs) were obtained by, and are available from, Genea Biosciences (http://geneabiocells.com/services/shelf-products/human-embryonic-stem-cells): WT019, WT022, HD018, HD020, HD089, HD090 (See Supplemental Table S1). Human fibroblasts (GM4204, GM04212, and GM09197) were obtained from Coriell and reprogrammed into iPSCs to obtain four independent lines (see Supplemental Table S2).

Cell Culture and Neuronal Differentiation

hESCs [14] and hiPSCs were cultured as described [15]. For neuronal induction, hiPSC colonies were induced for neuronal lineage differentiation using dual SMAD inhibition by blocking BMP and TGFβ. hiPSC colonies were separated and seeded on Matrigel as single cells and incubated with human induction media [DMEM/F12, Neurobasal, N2, B27] supplemented with 2 SMADi (20 μM SB, 100 nM LDN) and 1 μM XAV-939 for 10 days. From day 10 to 20 of differentiation, cells were incubated with neural patterning media supplemented with 50 nM SAG and 1 μM XAV-939, inducing the cells to become neural progenitor cells (NPCs). For neuronal differentiation, the cells were reseeded on PLO/laminin-coated plates at 75,000 cells/cm^2 and exposed to neuronal differentiation medium supplemented with 20 ng/ml BDNF, 0.5 mM dbcAMP, and 0.5 mM Valpromide.

Lentiviral Production and Neural Infection

HEK293T cells were transduced with the target lentiviral vector (either lenti-GFP-LMNA or lenti-GFP-progerin) (kind gift from Tom Misteli) and packaging vectors deltaR8.9 and VSV-G (2th generation) using TransIT-LT1 (Mirus) transfection reagent. Before transfection, HEK293T medium was replaced with neural medium (w/o neurofactors). Twenty-four- and 48-h post transfection, Polybrene (8 μg/ml) and neurofactors were added to filtered medium containing virions. From each well containing neurons, 2/3 of the volume was replaced with media containing virions for infection of the neurons.

Immunofluorescence and Immunohistochemistry

For immunofluorescence (IF), cells were fixed in 4% Paraformaldehyde (PFA), permeabilized with 0.5% Triton X-100, and blocked with 5% fetal bovine serum (FBS). For immunohistochemistry, mice were sacrificed 5 months after transplantation, and brains were extracted, and incubated in 4% PFA overnight. Hippocampus and striatum were sectioned to 100 μM coronal sections. Primary antibodies were incubated overnight at 4 °C. Appropriate Alexa 488-, 568-, or 647-conjugated secondary antibodies were diluted 1:10,000 and mixed with DAPI. Images were acquired using an Olympus IX81 epifluorescence microscope and analyzed and processed using ImageJ. The following primary antibodies were used: MAP2 (Sigma M1406, 1:200), GAD65/67 (Abcam, AB1511, 1:200), HTT (Millipore MAB2166, 1:500), DARPP32 (Abcam ab40801), Nestin (Santa-Cruz, sc-21248, 1:100), SOX2 (Cell Signaling #2748, 1:100), and PAX6 (Covance PRB-278P, 1:200). The secondary antibodies were goat anti-rabbit or mouse IgG conjugated with Alexa-488, Alexa-594, or Alexa-647 (Invitrogen).

Mice

Adult, 16-week-old male severe combined immuno-deficient (SCID) mice were anesthetized with Ket/Xyl mixture according to body weight. Following anesthesia, mice were injected s.c. with Rimadyl (pain killer) according to body weight. Following hair removal, ethanol disinfection of the head, and skull hole drill, mice received a stereotaxic injection of 2 μl of 0.1 M quinolinic acid (QA, P63204; Sigma, in PBS) using 32 ga needle into the right striatum using stereotaxic apparatus (coordinates AP = + 0.8 mm rostral, ML = + 2.0 mm, DV = − 3.2 mm). After the injection, the hole in the skull was filled with Bone Wax and the skin was stitched with silk fabric in a "stitch-knot-cut" method. At the end of the surgery, an isotonic solution (NaCl/glucose, 600 μl) was

injected i.p. Mice were kept warm using a red lamp. Mice were monitored throughout the experiment. Six weeks after the QA, neuronal lineage cells at differentiation day 24 (50,000 cells/μl in neural patterning media) were injected (2 μl) into the injured striatum (AP = + 0.8 mm, L = + 2.0 mm, V = − 3.2 mm) of anesthetized mice with a 24 ga needle over a period of 5 min. Mice were sacrificed 5 months thereafter. Mice' brains were sectioned and stained with human specific markers together with neuronal markers. The Hebrew University is an AAALAC International accredited institute. All animal experiments were conducted in accordance with the Hebrew University's animal committee, ethical approval number IACUC: NS-14444-3.

Electrophysiology

For electrophysiological recordings, cultures were grown on cover glass (Marienfeld, ⌀12 mm). Prior to the recordings, the medium was replaced with an artificial cerebrospinal fluid (ACSF) containing 126 mM NaCl, 2.5 mM KCl, 1.25 mM NaH_2PO_4, 2 mM $MgSO_4$, 10 mM glucose, 26 mM $NaHCO_3$, and 2 mM $CaCl_2$. For blocking $GABA_A$ receptors, the ACSF was replaced with an ACSF of the same content but with 100 μM Picrotoxin. For local administration of GABA, a pipette with large opening was filled with ACSF with 500 μM GABA and was placed at the distance of 20–50 μm from the recorded cell; the pressure was controlled using a custom built system. The cultures were transferred to a recording chamber, where ACSF was continuously superfused with ACSF bubbled with 95% O_2 and 5% CO_2 (pH 7.3–7.5). The recordings were made at room temp. Recording pipettes were pulled from borosilicate glass using Narishige PP-830 puller to resistance of 4–10 MΩ and filled with an intracellular solution containing 130 mM K-gluconate, 2 mM Na-gluconate, 6 mM NaCl, 2 mM $MgCl_2$, 10 mM HEPES, 14 mM Tris-phosphocreatine, 4 mM MgATP, 0.3 mM Tris-GTP, 1 mM EGTA, 10 mM sucrose, and 25 μM Alexa Fluor 594 (pH 7.29 with KOH). Cells were identified under an infrared-DIC microscope (Olympus BX61WI) using a 20× Olympus objective. Recordings were done using Axoclamp 700B amplifier and digitized with National Instruments data acquisition board controlled by a custom built software developed in Labview. Data were analyzed using Python and R.

Bioinformatic Analysis

RNA and Preprocessing of RNA-Seq Raw Sequencing Data

RNA was extracted from neurons using Qiagene 96-well kit according to the manufacturer's instructions. RNA concentration was determined using Qubit in an automated plate reader, and 15 ng RNA from each sample in 15 μl total volume was taken for RNA-seq. DGE raw reads from 96-well plates were first demultiplexed according to their barcode using novobarcode script from the NovoAlign package (Novocraft) using distance = 3 parameter. Single-end reads were then mapped to the human genome (hg19) using the STAR aligner [16] with parameters alignIntronMax = 1000 and alignMatesGapMax = 1000. Unmapped reads and reads with quality score < 10 for any of the positions in the sequence were discarded and multiple reads with the same UMI in the same sample were removed. Filtered reads were then passed to the End Sequence Analysis Toolkit (ESAT) [17] to correct for computational artifacts in the DGE method, with parameters wLen = 400, wOlap = 50, wExt = 2000, and sigTest = 0.05. Low-quality samples were removed based on the number of aligned reads if they had less than 200,000 reads. This threshold also corresponded to samples with low number of detected genes. Cell lines which did not have at least two biological replicates (after filtering out low quality samples) were discarded from the analysis. Finally, reads were normalized based on quantiles, resulting in normalized reads per million (RPM) values.

Gene Expression Analysis

In order to find differentially expressed (DE) genes between WT and HD cell lines, outlier expression values were first removed for each gene using the MAD criterion (i.e., if one normalized count was more than 4 MADs away from the median expression value of that gene, it was removed from the analysis). Then, a two-tailed *t* test was applied for all genes, which had a mean expression of more than 5 normalized RPM counts in the WT or HD samples. Genes were considered consistent if they were significantly (p value < 0.05) up-(/down-) regulated at least 2-fold in hESC samples, and 1.5-fold in iPSC samples, or vice versa. Gene ontology (GO) analysis for DE genes was performed using PANTHER (http://pantherdb.org/) over-representation test [18].

Results

In order to study HD-related transcriptional changes, we took advantage of both WT and HD hESCs and hiPSCs, and developed a rapid and robust GABAergic differentiation protocol. We used six cell lines of previously characterized WT and HD hESCs [14], as well as four iPSC lines that we generated by reprogramming fibroblasts from three human subjects carrying expanded CAG repeats in the *HTT* gene, from the Coriell Repository (See Supplemental Tables S1 and S2 for cell lines and genotyping, and Fig. S1 for hiPSC characterization). Cells were dissociated into single cells using accutase and incubated with neural induction medium containing dual SMAD inhibitors (SB431542; LDN193189, as an alternative small molecule

to Noggin, which selectively inhibits BMP signaling) [19–21] as well as the small molecule DKK1-analog XAV-939, which inhibits Wnt signaling [20, 21] (Fig. 1a). XAV-939 blocks the poly-ADP ribosylation activity of Tankyrase, thereby stabilizing Axin and promoting β-catenin degradation [22]. Cells were treated with the three inhibitors for 10 days, while changing medium every other day (Fig. 1b, c). At day 10 (Fig. 1d), media was replaced with neural patterning media containing XAV-939 and SAG (Smoothened/Smo agonist), a potent small molecule activator of Sonic hedgehog (Shh) signaling [23]. We also tested other Smo agonists/Shh activators, including GSA10 and Purmorphamine [10, 24], but both were found to be less effective than SAG in promoting neurogenesis, according to cellular morphology at early stages of differentiation (days 10–20), and according to survival upon transition from neural progenitor cells into neurons. Between days 10–20, the cells proliferate and gain different morphologies including rosette structures (Fig. 1e). At day 20, the cells become neuronal progenitor cells and express NESTIN, PAX6 and SOX2 (Fig. S1c, d).

Existing GABAergic differentiation protocols use either rosette picking/colony picking or sorting by FACS or MACS at the stage of neuronal progenitor cells (NPCs) in order to filter the non-neuronal cells from the mixed population of cells. These methods result in relatively low viability of the picked cells, and limited amounts of neuronal progenitors upon transfer. Hence, on day 20–22, we reseeded the cells on Poly-L-ornithine (PLO)/Laminin coated plates, promoting neural stem/progenitor cell differentiation via ERK signaling [25]. The detachment step further ensures that only living

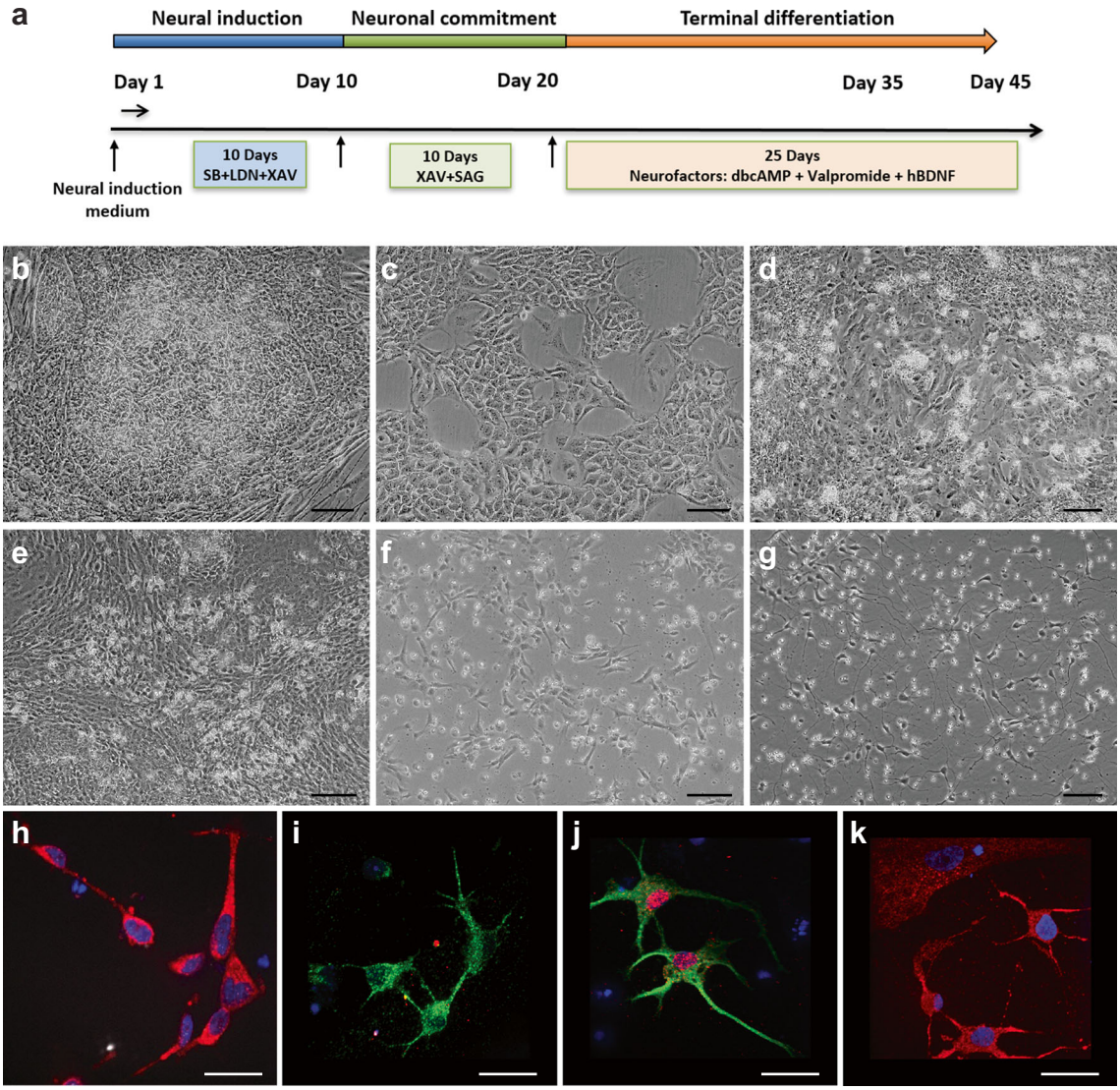

Fig. 1 From hPSC to GABAergic neurons. **a** A schematic diagram of the differentiation process. **b** hPSC colony on mitomycin-treated MEFS. **c** Differentiation day 1. **d** Differentiation day 10. **e** Differentiation day 15. **f** Differentiation day 21. **g** Differentiation day 35–42. Scale bars in **b**–**g** = 50 μm. **h**–**k** Striatal GABAergic cells were stained with antibodies for MAP2 (**h**, red); GAD65 (**i**, green); DARPP32 and MAP2 (**j**, red and green respectively) and HTT (**k**, red). DAPI, blue in **h** and **k**. Scale bars in **h**–**k** = 10 μm

proliferating cells adhere to the new matrix. One day after seeding (day 21), the cells show neuronal progenitor cells morphology (Fig. 1f).

To improve differentiation yield, we tested various published and unpublished combinations of neurofactors with different neuronal differentiation media, and found that a previously published medium (DMEM/F12:Neurobasal with N2, B27, bME, 1/2 PenStrep) [10] supplemented with dVB (0.5 mM dbcAMP, 0.5 mM Valpromide, 25 ng/ml hBDNF) was most effective. Comparing the histone deacetylase (HDAC) inhibitor valproic acid (VPA) and Valpromide (VPM), a structural analog of VPA, we found that Valpromide is significantly more effective in our conditions. Dibutyryl-cAMP (dbcAMP), a cell permeable analogue of cAMP, which is widely used in neuronal differentiation protocols, inhibits neuronal glucose uptake via PKA activation [26]. VPM and dbcAMP induce terminal neuronal differentiation in concert with human brain-derived neurotrophic factor (hBDNF), a member of the neurotrophin growth factor family that binds and activates TrkB and p75 neurotrophin receptors, promoting survival, growth, and differentiation of neurons [27]. We grew our cells in these conditions for additional 13–15 days. On differentiation day 35 to 45, cells were post-mitotic, exhibited neuronal morphology (Fig. 1g) and expressed neuronal, GABAergic, and striatal markers (Fig. 1h, k). Importantly, both WT and HD hPSCs differentiated successfully into GABAergic neurons with no apparent differences. We examined the reproducibility of this protocol by conducting more than ten independent biological experiments, each one with at least three biological replicates, using different hPSC lines. Differentiation efficiency was consistent throughout different cell lines based on neuronal number and morphology at the end of the differentiation process, as well as immunofluorescence quantification of neuronal, striatal, and GABAergic markers.

To test the validity of our generated neurons, we first verified that our neurons possess electrical activity. We performed whole cell intracellular recordings in 39 differentiated cells filled with Alexa594 under a DIC microscope (Fig. 2a). Eighteen cells (46%) had action potentials, either spontaneous (Fig. 2b) or evoked (Fig. 2c). In addition, in 10 of the non-spiking cells, voltage-dependent channels were observed (Fig. 2d), suggesting neuronal commitment, albeit immature. The measured passive membrane properties (membrane input resistance and membrane time constant) were distributed in a wide range, similar to previous reports [10], and spike amplitudes were in the expected range, between 20 and 80 mV. Comparative membrane potential fluctuations analysis [28] showed reduction in membrane fluctuations when $GABA_A$ receptors were blocked by picrotoxin (PTX, Fig. 2e), supporting the presence of GABA signaling in the culture. In addition, we validated the expression of $GABA_A$ receptors by recording currents following local application of GABA

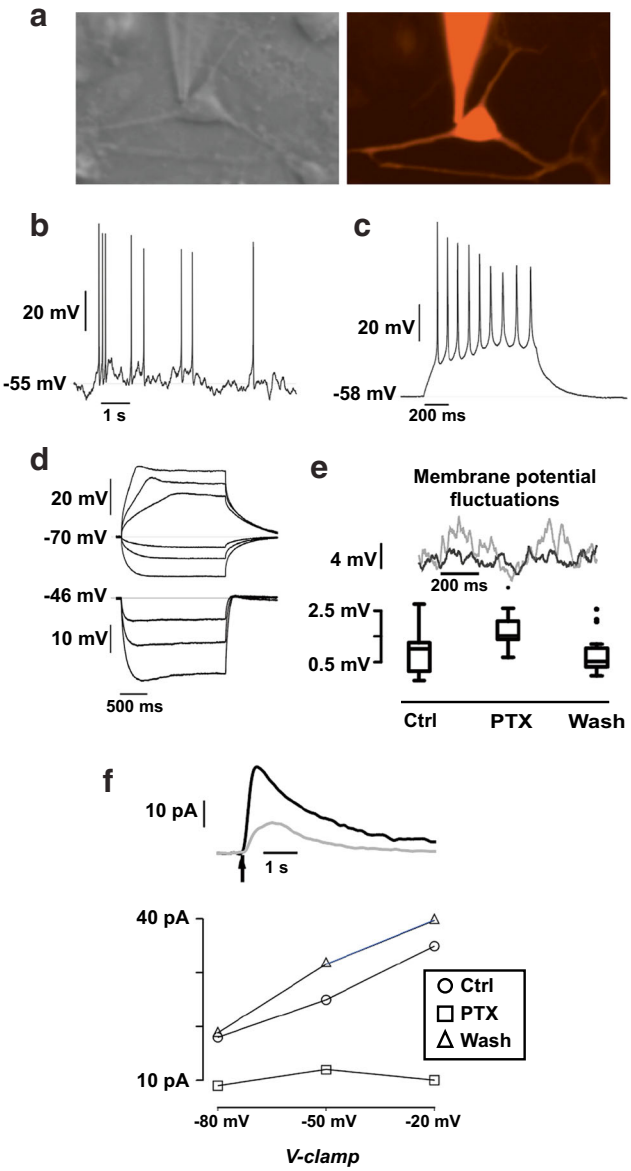

Fig. 2 Electrophysiological characterization of PSC-derived striatal GABAergic neurons. **a** Representative DIC (left) and fluorescent (right) images during electrical recordings. **b**, **c** Representative whole cell intracellular recording of spontaneous (**a**) or evoked (**b**) neuronal activity. **d** Subthreshold response demonstrating the presence of voltage-dependent channels in non-firing cells. **e** Membrane potential fluctuations analysis following picrotoxin (PTX) administration. *Top*: 1 s segments of CTL (black) and PTX (gray) conditions, *bottom*: representative distribution of fluctuation amplitude of 1 s segments in 40 s traces ($n = 40$ for each condition). The differences between CTL and PTX and between PTX and WSH aresignificant ($p < 0.001$, Mann-Whitney-Wilcoxon U test). **f** Response to GABA local administration. *Top*: during CTL (black) and PTX (gray) in voltage clamp (− 20 mV) mode; *bottom*: amplitude of current transients induced by local GABA administration at varying holding potentials in voltage clamp

(Fig. 2f). These results suggest that > 40% of our cultured neurons reached electrophysiological maturation, and that at least some of our post-mitotic neurons express GABA receptors. Together with the expression of striatal GABAergic

markers (Fig. 1h, k and Fig. S3), we conclude that a large fraction of these post-mitotic neurons are GABAergic. As a final validation experiment, we transplanted our PSC-derived neurons in vivo. We stereotactically transplanted the neurons into Quinolinic Acid (QA) treated mice [9, 10, 20]. Six months thereafter, we sacrificed the animals, sectioned their brains, and stained for human markers. We found evidence for clusters of both WT and HD human neurons in the mouse striatum (Fig. S2a), attesting to the capacity of the cells to integrate in vivo [29], with no evidence for tumor formation in any of the transplanted mice.

Next, we compared transcriptomes of WT (029 cell line) and HD (090 HD line) hESC-derived GABAergic neurons using digital gene expression RNA-seq (DGE). Interestingly, although long polyQ repeats were shown to impede neuronal differentiation [30], we found only a few significant changes of differentially expressed genes (DEGs) between HD and WT hESC-derived neurons (Fig. 3a top). The pathological effects in different neurodegenerative chronic diseases only begins at an older age. One of the major limitations of modeling late-onset neurodegenerative diseases using PSCs is that the neurons produced from embryonic or reprogrammed cells are presumably young, whereas their in vivo counterparts are old. To recapitulate aging in our HD models, we first tried glutamate excitation (100 μM), as described [31], but found no apparent differences in the cells' morphology, HTT expression, or GABAergic and neuronal marker expression in general (data not shown). We therefore used ectopic expression of Progerin, a truncated form of Lamin A (LMNA) caused by a splice-site mutation resulting in Hutchinson Gilford Progeria Syndrome [32, 33]. Progerin was previously shown to effectively accelerate aging in cultured neurons in a dominant negative fashion, enabling modeling of late-onset Parkinson's disease [13]. We first expressed lenti-GFP-LMNA and lenti-GFP-Progerin in WT and HD patient-derived primary fibroblasts. As expected, Progerin-expressing nuclei showed wrinkled morphology (Fig. 4a). We then switched to post-mitotic neurons, and infected them with lenti-GFP-Progerin 6 days before the end of our neuronal differentiation protocol. We infected the cells twice, with a highly efficient transduction rate of over 90%. Within 48 h, Progerin-expressing ("aged") cells displayed significant nuclear membrane folding and blebbing (Fig. 4b), as observed in "aged" cells, while the membrane of GFP-LMNA expressing cells was intact. Progerin-expressing cells displayed normal marker expression and electrophysiological properties. At the transcriptional level, when we compared Progerin-infected post-mitotic neurons with unaffected neurons, we found that differentially expressed genes were enriched for genes involved in double-strand break repair, DNA packaging, DNA helicase activity, and collagen binding (Supplemental Table S3), consistent with observations that Progerin causes an oxidative stress that inflicts DNA damage [34–36].

Next, we compared the transcriptome expression upon aging, in "aged" HD versus "aged" WT neurons (both expressing Progerin). Progerin-induced aging resulted in almost 2-

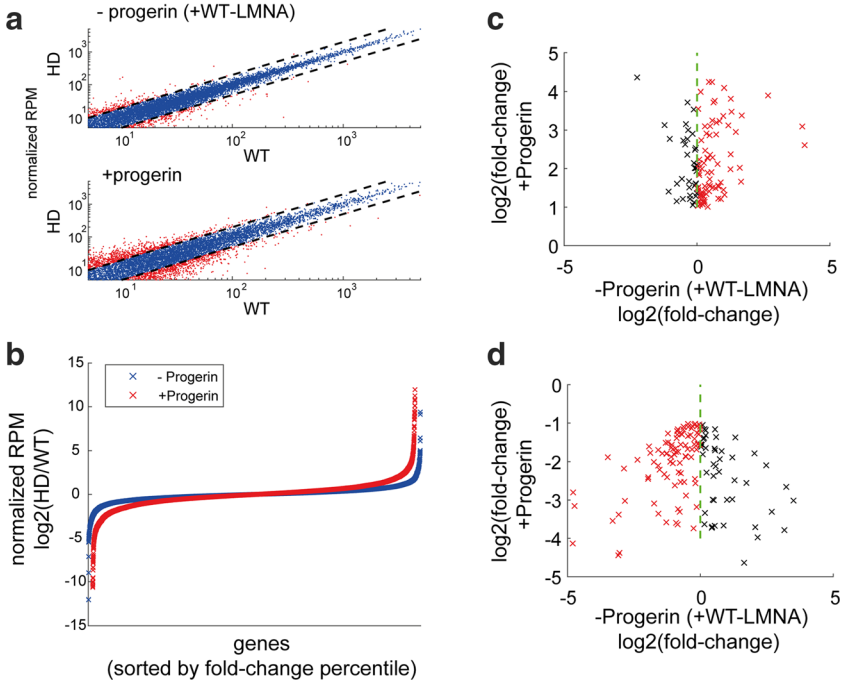

Fig. 3 Progerin affects nuclear morphology of human fibroblasts and post-mitotic neurons. **a** Left: nuclear morphology in WT-LMNA-GFP expressing fibroblasts. HP1γ is shown in red. Right: nuclear morphology in Progerin-GFP expressing fibroblasts. HP1γ is shown in red. **b** Nuclear morphology in Progerin-GFP expressing WT (top) and HD (bottom) iPSC-derived neurons. GAD65 is shown in red. Scale bar = 10 μm

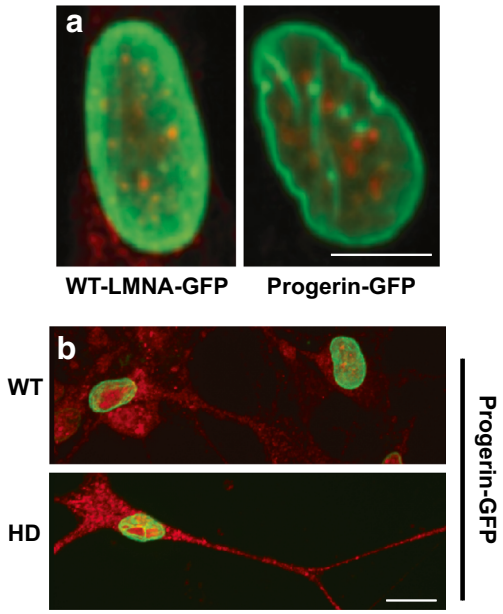

Fig. 4 Progerin enhances HD-associated gene expression changes in terminally differentiated neurons. **a** Mean expression of genes in HD cells compared to WT cells expressing WT-GFP-LMNA (top) or GFP-Progerin (bottom). Dashed lines represent 2-fold difference. Red dots denote the differentially expressed genes. **b** Sorted values of the fold change of all expressed genes between HD and WT cells, expressing either WT-GFP-LMNA (blue) or GFP-Progerin (red). **c**, **d** Fold change of upregulated (**c**) and downregulated (**d**) genes between HD and WT cells expressing either WT-GFP-LMNA (X-axes) or GFP-Progerin (Y-axes). Red, genes which are up- (/down-) regulated both with and without Progerin. Black, genes which have a different trend between HD and WT. The dashed line represents no change between HD and WT without Progerin. Note that in most cases, Progerin enhanced the already existing (although non-significant without Progerin) changes in gene expression

fold increase in the number of DEGs between HD and WT hPSC-derived neurons, from 176 (in "young" WT Vs. "young" HD) to 290 genes (in "aged" WT Vs. "aged" HD) (Fig. 3a, bottom and Fig. 3b). Interestingly, when we closely examined the 290 DEGs (in the "aged" WT Vs. the "aged" HD neurons), we noticed that many of them, including both upregulated (Fig. 3c) and downregulated (Fig. 3d) genes, already showed the same trend in the "young" neurons (i.e., in the "young" WT Vs. the "young" HD neurons), but these differences only became significant following the Progerin treatment. These genes were significantly enriched for genes related to the kinetochore and the mitotic spindle, as well as neuronal development (Supplemental Table S4). These results indicate that ectopic expression of Progerin can accelerate aging at the cellular level, and exacerbate late-onset disease relevant pathways.

To examine in a more rigorous way the aging-dependent differences between WT and HD, we conducted a larger scale RNA-seq experiment, which included both hESC- and iPSC-derived aged neurons from different cell lines. Clustering of the transcriptomes revealed that the origin of the derived cells, hESC or iPSC, had a major contribution to the transcriptional profile of the cells, which dominated over the Progerin effect (Fig. S2b). We therefore conducted the analysis for each of them separately. While no evident pathways were found among the 214 genes which were consistently and significantly differentially expressed in both hESC- and iPSC-derived neurons, separate gene annotation analysis revealed changes in genes related to generation of neurons, neurogenesis, nervous system development, and cell adhesion in hESC- as well as iPSC-derived neurons (Supplemental Table S5). This is consistent with previous reports of HD transcriptional changes in differentiated pluripotent cells [11, 37]. In addition, DEGs in iPSC-derived neurons were enriched for cilium organization while DEGs in hESC-derived neurons were enriched for synapse assembly and glutamatergic synaptic transmission, glutamate receptor signaling pathway, and axonogenesis (Supplemental Table S5). Ciliogenesis is regulated by the HTT protein [38] and is affected in HD [39], and glutamate receptor signaling has been also previously observed in HD [37]. Interestingly, we found that IGF1 and two of the six IGF binding proteins, IGFBP3 and IGFBP4, were consistently differentially expressed between WT and HD in hESC- and iPSC-derived neurons with Progerin treatment, where IGF1 and IGF4 were similarly expressed between WT and HD neurons without Progerin treatment. IGF1 levels correlate with the level of cognitive impairment in human [40], and IGF1 treatment has been shown to ameliorate disease phenotypes in HD mouse model [41]. Together with our data, this raises the possibility that IGF1 is involved in more advanced stages of the disease. Finally, GAD1, which is responsible for the production of GABA, was also significantly upregulated in HD neurons in both hESC- and iPSC-derived neurons.

Taken together, we established a convenient differentiation system to model HD using either human ESCs or iPSCs, demonstrated that the produced neurons are GABAergic and are electrophysiologically active, and showed that Progerin expression exacerbates the otherwise subtle changes in gene expression.

Discussion

In this study, we developed a rapid and reproducible, striatal GABAergic differentiation method for human pluripotent stem cells to effectively model and study Huntington's disease (HD). The ~45 days differentiation protocol, which is based on previously published protocols and was further optimized, is applicable to both human ESCs and patient-derived iPSCs and results in striatal GABAergic neurons. The resulting striatal post-mitotic neurons express GABAergic and striatal marker combinations, display electrophysiological properties of GABA receptor containing neurons, and are successfully grafted in vivo.

We used a combination of several previously published protocols, and through the use of small molecules and a variety of different inhibitors, we were able to improve existing yields and expedite the differentiation process. Dual SMAD inhibition was followed by a unique combination of neurofactors, which enabled fast and efficient striatal GABAergic differentiation. We also combined the use of XAV-939, which blocks the poly-ADP ribosylation activity of Tankyrase, thus stabilizing Axin and promoting β-catenin degradation [22]. Those three inhibitors together, combined with the later action of SAG (Smoothened/Smo agonist), which is a potent small molecule activator of Sonic hedgehog (Shh) signaling [23], resulted in a relatively robust and uniform differentiation. We note that optimal cell density is extremely important for obtaining optimal results. The differentiated cells show both spontaneous and evoked electrophysiological activity, as well as the presence of GABA signaling, both by administration of the $GABA_A$ antagonist picrotoxin (PTX), resulting in reduction of membrane fluctuations, and by direct local administration of GABA, which resulted in increased currents in response to increased voltage clamps. The neurons are also effectively engrafted in vivo and survive months following transplantation in QA-lesioned mice.

While most studies focused solely on patients' iPSCs, which are the most readily available source of mutant PSCs, here, we used a side-by-side comparison of both iPSCs and hESCs derived from PGD HTT mutant embryos [14]. We also used several different sources of iPSCs, as well as iPSCs carrying different polyQ lengths, to account for the inherent heterogeneity of the disease, the donors, and the differentiation system. These multiple sources of PSCs enabled us to identify very selective genes and pathways that are likely a result of the polyQ expansion mutation rather than the donor/cell of origin/culture and differentiation conditions, etc.

As expected from differentiated embryonic (ESCs) or "rejuvenated" (iPSCs) cells, we found very few differentially expressed genes between WT and HD neurons. However, when we ectopically expressed the mutant Δ50 lamin A protein (Progerin), which causes Hutchinson Gilford Progeria Syndrome (HGPS) in a dominant negative fashion [32, 33], the neurons were effectively aged in culture, as previously reported [13]. This aging protocol successfully enhanced the otherwise subtle changes observed in gene expression between WT and HD GABAergic neurons, and enabled the identification of differentially expressed genes, which show the same trends in all our cellular systems.

"Accelerated aging" using reactive oxygen species has been previously applied for several neurodegenerative disease cellular models, including Parkinson's, Alzheimer's disease, and schizophrenia [42]. Why do disease-related cellular alterations manifest mainly in old, and not young, neurons? The general accepted view is that aging is a multi-layered process involving epigenetic perturbations, senescence, telomere shortening, mtROS accumulation, DNA damage, all of which contribute to a gradual cellular damage, and the degeneration of neurons. In neurodegenerative diseases, the dysregulated proteins either accelerate the damage or abolish cellular repair mechanisms, and thereby contribute to neuronal death by different mechanisms.

Aging, as well as neurodegenerative diseases, was also shown to be associated with cellular senescence [43], suggesting that senescence is a part of the aging process, occurring in both neurons and glia. It has been previously shown that in the timeframe of Progerin expression (5 days), aging-related processes such as telomere shortening, modified gene expression, altered nuclear morphology and mtROS all take place [13]. Senescence was also tested using the β-galactosidase (β-GAL) assay, which is a common reporter for cellular senescence; however, no increased β-GAL activity was observed in the timeframe of the experiment. In our experiment, we also checked for changes in the transcriptional level for the other senescence genes including RB1, Rb2/p130, p16, and p53 in Progerin-expressing cells and found no significant changes [44].

Another possible alternative of using Progerin is direct trans-differentiation of fibroblasts from old donors, directly to mature neurons [45]. In this study, the authors used a 35-day protocol combining miR-9/9*-124, CTIP2, DLX1, DLX2, and MYT1L (CDM) to generate striatal medium spiny neurons in culture. Unlike PSC-derived neurons, trans-differentiated neurons, which originated from HD patients, showed cellular polyQ aggregates and other HD-related phenotypes, e.g., mitochondrial dysfunction and spontaneous degeneration over time, compared with neurons obtained from healthy samples [46]. One notable disadvantage of trans-differentiation is the varied "age" of the differentiated neurons, as trans-differentiation maintain the aging-related traits, and the age of the donor affects the disease phenotype [47]. In contrast, hiPSC-derived neurons, in which reprogramming erases all epigenetic marks, re-acquire them upon differentiation, and Progerin can reset them all to the same age in culture. Thus, by applying hPSC-derived neurons expressing Progerin, it is possible to generate neurons which originated from different donors, but shows a uniform epigenetic signature. Overall, our study offers a robust method for human PSCs differentiated GABAergic neurons for efficient modeling of HD and other diseases. Ectopic expression of Progerin enabled us to identify unique HD transcriptional changes, which occur before any irreversible neurological function loss, representing pre-symptomatic clinical stages. Exploring pre-symptomatic stages may not only shed light on early mechanistic cellular pathways leading to neuronal degeneration and death, but may also lead to early prevention.

Author Contributions D. Cohen-Carmon, M. Sorek, V. Lerner, Y. Yarom, and E. Meshorer designed the research; D. Cohen-Carmon, M. Sorek, V. Lerner, and M. Nissim-Rafinia performed the research; D. Cohen-Carmon, M. Sorek, and V. Lerner analyzed the data; Cohen-Carmon, M. Sorek, and E. Meshorer wrote the paper.

Funding Information The work was supported by the Israel Science Foundation (1140/17 to E.M.), a TEVA National Network of Excellence award (to E.M. and D.C.C), and the Azrieli Foundation Fellowship (to M.S.).

Data Availability All data are available at through GEO (GSE111622).

References

1. Milnerwood AJ, Raymond LA (2010) Early synaptic pathophysiology in neurodegeneration: insights from Huntington's disease. Trends Neurosci 33(11):513–523. https://doi.org/10.1016/j.tins.2010.08.002
2. Andrew SE, Goldberg YP, Kremer B, Telenius H, Theilmann J, Adam S, Starr E, Squitieri F et al (1993) The relationship between trinucleotide (CAG) repeat length and clinical features of Huntington's disease. Nat Genet 4(4):398–403. https://doi.org/10.1038/ng0893-398
3. Myers RH, MacDonald ME, Koroshetz WJ, Duyao MP, Ambrose CM, Taylor SA, Barnes G, Srinidhi J et al (1993) De novo expansion of a (CAG)n repeat in sporadic Huntington's disease. Nat Genet 5(2):168–173. https://doi.org/10.1038/ng1093-168
4. Pouladi MA, Morton AJ, Hayden MR (2013) Choosing an animal model for the study of Huntington's disease. Nat Rev Neurosci 14(10):708–721. https://doi.org/10.1038/nrn3570
5. Chen Y, Carter RL, Cho IK, Chan AW (2014) Cell-based therapies for Huntington's disease. Drug Discov Today 19(7):980–984. https://doi.org/10.1016/j.drudis.2014.02.012
6. Jung YW, Hysolli E, Kim KY, Tanaka Y, Park IH (2012) Human induced pluripotent stem cells and neurodegenerative disease: prospects for novel therapies. Curr Opin Neurol 25(2):125–130. https://doi.org/10.1097/WCO.0b013e3283518226
7. Halevy T, Urbach A (2014) Comparing ESC and iPSC-based models for human genetic disorders. J Clin Med 3(4):1146–1162. https://doi.org/10.3390/jcm3041146
8. Connor B (2018) Concise review: the use of stem cells for understanding and treating Huntington's disease. Stem Cells 36(2):146–160. https://doi.org/10.1002/stem.2747
9. Aubry L, Bugi A, Lefort N, Rousseau F, Peschanski M, Perrier AL (2008) Striatal progenitors derived from human ES cells mature into DARPP32 neurons in vitro and in quinolinic acid-lesioned rats. Proc Natl Acad Sci U S A 105(43):16707–16712. https://doi.org/10.1073/pnas.0808488105
10. Ma L, Hu B, Liu Y, Vermilyea SC, Liu H, Gao L, Sun Y, Zhang X et al (2012) Human embryonic stem cell-derived GABA neurons correct locomotion deficits in quinolinic acid-lesioned mice. Cell Stem Cell 10(4):455–464. https://doi.org/10.1016/j.stem.2012.01.021
11. Consortium HDi (2012) Induced pluripotent stem cells from patients with Huntington's disease show CAG-repeat-expansion-associated phenotypes. Cell Stem Cell 11(2):264–278. https://doi.org/10.1016/j.stem.2012.04.027
12. Delli Carri A, Onorati M, Lelos MJ, Castiglioni V, Faedo A, Menon R, Camnasio S, Vuono R et al (2013) Developmentally coordinated extrinsic signals drive human pluripotent stem cell differentiation toward authentic DARPP-32+ medium-sized spiny neurons. Development 140(2):301–312. https://doi.org/10.1242/dev.084608
13. Miller JD, Ganat YM, Kishinevsky S, Bowman RL, Liu B, Tu EY, Mandal PK, Vera E et al (2013) Human iPSC-based modeling of late-onset disease via progerin-induced aging. Cell Stem Cell 13(6):691–705. https://doi.org/10.1016/j.stem.2013.11.006
14. Bradley CK, Scott HA, Chami O, Peura TT, Dumevska B, Schmidt U, Stojanov T (2011) Derivation of Huntington's disease-affected human embryonic stem cell lines. Stem Cells Dev 20(3):495–502. https://doi.org/10.1089/scd.2010.0120
15. Takahashi K, Tanabe K, Ohnuki M, Narita M, Ichisaka T, Tomoda K, Yamanaka S (2007) Induction of pluripotent stem cells from adult human fibroblasts by defined factors. Cell 131(5):861–872. doi:S0092-8674(07)01471-7. https://doi.org/10.1016/j.cell.2007.11.019
16. Dobin A, Davis CA, Schlesinger F, Drenkow J, Zaleski C, Jha S, Batut P, Chaisson M et al (2013) STAR: ultrafast universal RNA-seq aligner. Bioinformatics 29(1):15–21. https://doi.org/10.1093/bioinformatics/bts635
17. Derr A, Yang C, Zilionis R, Sergushichev A, Blodgett DM, Redick S, Bortell R, Luban J et al (2016) End sequence analysis toolkit (ESAT) expands the extractable information from single-cell RNA-seq data. Genome Res 26(10):1397–1410. https://doi.org/10.1101/gr.207902.116
18. Mi H, Huang X, Muruganujan A, Tang H, Mills C, Kang D, Thomas PD (2017) PANTHER version 11: expanded annotation data from gene ontology and Reactome pathways, and data analysis tool enhancements. Nucleic Acids Res 45(D1):D183–D189. https://doi.org/10.1093/nar/gkw1138
19. Chambers SM, Fasano CA, Papapetrou EP, Tomishima M, Sadelain M, Studer L (2009) Highly efficient neural conversion of human ES and iPS cells by dual inhibition of SMAD signaling. Nat Biotechnol 27(3):275–280. https://doi.org/10.1038/nbt.1529
20. Nicoleau C, Varela C, Bonnefond C, Maury Y, Bugi A, Aubry L, Viegas P, Bourgois-Rocha F et al (2013) Embryonic stem cells neural differentiation qualifies the role of Wnt/beta-catenin signals in human telencephalic specification and regionalization. Stem Cells 31(9):1763–1774. https://doi.org/10.1002/stem.1462
21. Matsuda K, Kondoh H (2014) Dkk1-dependent inhibition of Wnt signaling activates Hesx1 expression through its 5′ enhancer and directs forebrain precursor development. Genes Cells 19(5):374–385. https://doi.org/10.1111/gtc.12136
22. Huang SM, Mishina YM, Liu S, Cheung A, Stegmeier F, Michaud GA, Charlat O, Wiellette E et al (2009) Tankyrase inhibition stabilizes axin and antagonizes Wnt signalling. Nature 461(7264):614–620. https://doi.org/10.1038/nature08356
23. Chen JK, Taipale J, Young KE, Maiti T, Beachy PA (2002) Small molecule modulation of smoothened activity. Proc Natl Acad Sci U S A 99(22):14071–14076. https://doi.org/10.1073/pnas.182542899
24. Gorojankina T, Hoch L, Faure H, Roudaut H, Traiffort E, Schoenfelder A, Girard N, Mann A et al (2013) Discovery, molecular and pharmacological characterization of GSA-10, a novel small-molecule positive modulator of smoothened. Mol Pharmacol 83(5):1020–1029. https://doi.org/10.1124/mol.112.084590
25. Ge H, Tan L, Wu P, Yin Y, Liu X, Meng H, Cui G, Wu N et al (2015) Poly-L-ornithine promotes preferred differentiation of neural stem/progenitor cells via ERK signalling pathway. Sci Rep 5:15535. https://doi.org/10.1038/srep15535
26. Prapong T, Uemura E, Hsu WH (2001) G protein and cAMP-dependent protein kinase mediate amyloid beta-peptide inhibition of neuronal glucose uptake. Exp Neurol 167(1):59–64. https://doi.org/10.1006/exnr.2000.7519
27. Chao MV (2003) Neurotrophins and their receptors: a convergence point for many signalling pathways. Nat Rev Neurosci 4(4):299–309. https://doi.org/10.1038/nrn1078
28. Chorev E, Yarom Y, Lampl I (2007) Rhythmic episodes of subthreshold membrane potential oscillations in the rat inferior olive

nuclei in vivo. J Neurosci 27(19):5043–5052. https://doi.org/10.1523/JNEUROSCI.5187-06.2007
29. West EL, Gonzalez-Cordero A, Hippert C, Osakada F, Martinez-Barbera JP, Pearson RA, Sowden JC, Takahashi M et al (2012) Defining the integration capacity of embryonic stem cell-derived photoreceptor precursors. Stem Cells 30(7):1424–1435. https://doi.org/10.1002/stem.1123
30. Conforti P, Besusso D, Bocchi VD, Faedo A, Cesana E, Rossetti G, Ranzani V, Svendsen CN et al (2018) Faulty neuronal determination and cell polarization are reverted by modulating HD early phenotypes. Proc Natl Acad Sci U S A 115(4):E762–E771. https://doi.org/10.1073/pnas.1715865115
31. Koch P, Breuer P, Peitz M, Jungverdorben J, Kesavan J, Poppe D, Doerr J, Ladewig J et al (2011) Excitation-induced ataxin-3 aggregation in neurons from patients with Machado-Joseph disease. Nature 480(7378):543–546. https://doi.org/10.1038/nature10671
32. Eriksson M, Brown WT, Gordon LB, Glynn MW, Singer J, Scott L, Erdos MR, Robbins CM et al (2003) Recurrent de novo point mutations in lamin A cause Hutchinson-Gilford progeria syndrome. Nature 423(6937):293–298. https://doi.org/10.1038/nature01629
33. Meshorer E, Gruenbaum Y (2008) Rejuvenating premature aging. Nat Med 14(7):713–715. doi:nm0708-713. https://doi.org/10.1038/nm0708-713
34. Sieprath T, Darwiche R, De Vos WH (2012) Lamins as mediators of oxidative stress. Biochem Biophys Res Commun 421(4):635–639. https://doi.org/10.1016/j.bbrc.2012.04.058
35. Skoczynska A, Budzisz E, Dana A, Rotsztejn H (2015) New look at the role of progerin in skin aging. Menopause Review-Przeglad Menopauzalny 14(1):53–58. https://doi.org/10.5114/pm.2015.49532
36. Liu B, Wang J, Chan KM, Tjia WM, Deng W, Guan X, Huang JD, Li KM et al (2005) Genomic instability in laminopathy-based premature aging. Nat Med 11(7):780–785. https://doi.org/10.1038/nm1266
37. Lim RG, Salazar LL, Wilton DK, King AR, Stocksdale JT, Sharifabad D, Lau AL, Stevens B et al (2017) Developmental alterations in Huntington's disease neural cells and pharmacological rescue in cells and mice. Nat Neurosci 20(5):648–660. https://doi.org/10.1038/nn.4532
38. Saudou F, Humbert S (2016) The biology of Huntingtin. Neuron 89(5):910–926. https://doi.org/10.1016/j.neuron.2016.02.003
39. Keryer G, Pineda JR, Liot G, Kim J, Dietrich P, Benstaali C, Smith K, Cordelieres FP et al (2011) Ciliogenesis is regulated by a huntingtin-HAP1-PCM1 pathway and is altered in Huntington disease. J Clin Investig 121(11):4372–4382. https://doi.org/10.1172/Jci57552
40. Saleh N, Moutereau S, Azulay JP, Verny C, Simonin C, Tranchant C, El Hawajri N, Bachoud-Levi AC et al (2010) High insulinlike growth factor I is associated with cognitive decline in Huntington disease. Neurology 75(1):57–63. https://doi.org/10.1212/WNL.0b013e3181e62076
41. Lopes C, Ribeiro M, Duarte AI, Humbert S, Saudou F, de Almeida LP, Hayden M, Rego AC (2014) IGF-1 intranasal administration rescues Huntington's disease phenotypes in YAC128 mice. Mol Neurobiol 49(3):1126–1142. https://doi.org/10.1007/s12035-013-8585-5
42. Campos PB, Paulsen BS, Rehen SK (2014) Accelerating neuronal aging in in vitro model brain disorders: a focus on reactive oxygen species. Front Aging Neurosci 6:292. https://doi.org/10.3389/fnagi.2014.00292
43. Tan FCC, Hutchison ER, Eitan E, Mattson MP (2014) Are there roles for brain cell senescence in aging and neurodegenerative disorders? Biogerontology 15(6):643–660. https://doi.org/10.1007/s10522-014-9532-1
44. Alessio N, Capasso S, Ferone A, Di Bernardo G, Cipollaro M, Casale F, Peluso G, Giordano A et al (2017) Misidentified human gene functions with mouse models: the case of the retinoblastoma gene family in senescence. Neoplasia 19(10):781–790. https://doi.org/10.1016/j.neo.2017.06.005
45. Victor MB, Richner M, Hermanstyne TO, Ransdell JL, Sobieski C, Deng PY, Klyachko VA, Nerbonne JM et al (2014) Generation of human striatal neurons by microRNA-dependent direct conversion of fibroblasts. Neuron 84(2):311–323. https://doi.org/10.1016/j.neuron.2014.10.016
46. Victor MB, Richner M, Olsen HE, Lee SW, Monteys AM, Ma C, Huh CJ, Zhang B et al (2018) Striatal neurons directly converted from Huntington's disease patient fibroblasts recapitulate age-associated disease phenotypes. Nat Neurosci 21(3):341–352. https://doi.org/10.1038/s41593-018-0075-7
47. Tang Y, Liu ML, Zang T, Zhang CL (2017) Direct reprogramming rather than ipsc-based reprogramming maintains aging hallmarks in human motor neurons. Front Mol Neurosci:10. https://doi.org/10.3389/fnmol.2017.00359